MATCH
Communications in Mathematical and in Computer Chemistry

MATCH Commun. Math. Comput. Chem. **70** (2013) 745-758

ISSN 0340 - 6253

Solution of the Webb Equation for Kinetics of Cholinesterase Substrate-Inhibition/Activation Using the Adomian Decomposition Method

Marko Goličnik

Institute of Biochemistry, Faculty of Medicine, University of Ljubljana,

Vrazov trg 2, 1000 Ljubljana, Slovenia

e-mail: marko.golicnik@mf.uni-lj.si

(Received February 25, 2013)

ABSTRACT

The Webb rate equation has been widely used to describe the kinetic behavior of substrate inhibition and activation for various cholinesterases. However, its use is limited to the rate *versus* substrate-concentration analysis, as the integrated Webb equation cannot be expressed in an explicit closed-form reformulation of the time-dependent solution. In this article, I construct explicit approximations to the solution of the Webb rate equation as a recursive series using the Adomian decomposition method. This decomposition method is an elegant technique to handle nonlinear differential equations effectively, and thus it has recently been widely used to solve this class of equations in the sciences and engineering. I demonstrate here that the algebraic nature of these approximations to the solution of the Webb equation makes progress-curve analysis through the integrated rate equation an attractive and useful alternative for the cholinesterases that can be simply performed using any optional standard nonlinear regression software.

1. INTRODUCTION

The construction of a reaction model is one of the first steps a biochemist takes following the discovery of a novel enzyme. Hence, kinetic tools are used to determine the sequence of substrate binding with the appropriate affinity constants and the rates at which the (enzyme-) substrate intermediates are converted to the products. The kinetics of enzyme-catalyzed reactions are typically characterized in terms of their initial rates, which are determined at various substrate concentrations. Thus, instead of the integration of the model rate equations and the extraction of the full information from entire time-courses of the reaction, the experimental data over the short period when no more than 10% of the substrate has been consumed can be used for the initial rate determination method. Hence, despite the obvious advantages of progress-curve analyses, and because of their very nature (reaction measurements are typically represented as time–concentration data, and not as rate–concentration data), most biochemists appear not to be aware of their applications. Also, explicit mathematical solutions for various reaction models are not available for fitting to time-course data using a spreadsheet with commercial nonlinear regression software (e.g., Excel, SigmaPlot, Kaleidagraph, Prism). However, attempts have recently been made to obtain appropriate explicit approximation solutions of the integrated Michaelis-Menten [1-3] and Haldane equations [4].

Various kinetic models have been proposed to describe the reaction mechanisms of the cholinesterases, which have Michaelis-Menten–like mechanisms only for low initial substrate concentrations, and either substrate inhibition or activation for higher initial concentrations. This behavior of the cholinesterases with an excess of substrate that does not follow Michaelis-Menten kinetics is usually explained with the reaction model as shown in Scheme 1 [5-7].

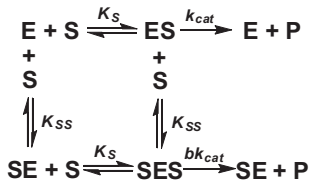

Scheme 1

This reaction model, in which the substrate molecule S binds to two different (active and peripheral) sites with two dissociation constants K_s and K_{ss}, can be used to describe both

substrate inhibition and activation at high substrate concentrations. These latter deviations from Michelis-Menten kinetics depend on parameter b in Scheme 1, which reflects the efficiency with which the ternary complex SES can form the product. The mathematical formalism of this enzyme reaction model was initially described by Webb [8] as:

$$v = \frac{d[P]}{dt} = -\frac{d[S]}{dt} = \frac{V_M[S]\left(1 + b\frac{[S]}{K_{SS}}\right)}{\left(K_S + [S]\right)\left(1 + \frac{[S]}{K_{SS}}\right)} \quad . \tag{1}$$

I therefore refer to Eq. (1) as the Webb equation, although some refer to it also as the Radić-Haldane equation [9]. In Eq. (1), V_M relates to the total enzyme concentration $[E]_T$ as $V_M = k_{cat}[E]_T$, and b determines the kinetic behavior. When b <1, there is substrate inhibition, when b >1, there is substrate activation, and if b = 1, the kinetics cannot be distinguished from Michaelis-Menten–like, as Eq. (1) then reformulates to give the classic Michaelis-Menten equation. Calculation of the solution to this Webb equation (Eq. (1)) demands numerical computation, as Eq. (1) can only be solved either by applying a general numerical integration technique for ordinary differential equations, or by a numerical root-finding method of the so-called integrated implicit form of Eq. (1), as:

$$\frac{\left([S]_0 - [S]_t\right)}{b} + K_S \ln\left(\frac{[S]_0}{[S]_t}\right) + \frac{(b-1)}{b^2}\left(bK_S - K_{SS}\right)\ln\left(\frac{K_{SS} + b[S]_t}{K_{SS} + b[S]_0}\right) = V_M t \tag{2}$$

Eq. (2) (for the derivation from Eq. (1) see the Appendix A) cannot be reformulated as an explicit closed-form equation like the integrated Michaelis-Menten equation [1,10-12]. However, recently, a great deal of interest has focused on the application of the Adomian decomposition method to the solving of a wide variety of nonlinear differential equations [13], whereby chemical kinetic problems are no exception [14]. The Adomian decomposition method has been applied for the last three decades as an iterative technique to obtain approximate analytical solutions of nonlinear differential equations that arise in various fields of the sciences and engineering. This method has also been offered recently as an alternative to the exact closed-form solution of the integrated Michaelis-Menten equation [2,3], which is expressed in terms of the non-elementary Lambert W(x) function. This technique, which provides approximate solutions in the form of power series, can efficiently compensate for the lack of W(x) in standard nonlinear regression software. Thus, in this article, I provide further

approximate solutions to more complex Webb rate equations for substrate inhibition/ activation enzyme kinetics that incorporate the use of the Adomian decomposition method.

2. THEORY

2.1. The Adomian decomposition method

In reviewing the Adomian decomposition methodology [13], we consider an initial-value differential equation:

$$\frac{du}{dt} + f(t,u) = 0, \qquad u(0) = u_0 \tag{3}$$

where f(t,u) is a nonlinear function that is analytic near u = u_0 and t = 0, and u_0 is an initial-condition data value. It is equivalent to solve the system of Eq. (3) and the Volterra integral equation:

$$u(t) = u_0 - \int_0^t f(s,u(s))ds \tag{4}$$

As usual in the Adomian decomposition method, the solution u(t) of Eq. (3) is considered to be the sum of a series:

$$u(t) = u_0 + \sum_{n=1}^{\infty} u_n \tag{5}$$

and the nonlinear function f(t,u) as the series of the function:

$$f(t,u) = \sum_{n=0}^{\infty} A_n\left(t, u_0, u_1, \cdots, u_n\right) \tag{6}$$

where A_n are the special Adomian polynomials that are obtained for the particular nonlinear function f(t,u). The A_n are given as:

$$\begin{aligned} A_0 &= f(u_0), \\ A_1 &= u_1 \frac{df(u_0)}{du_0}, \\ A_2 &= u_2 \frac{df(u_0)}{du_0} + \left(\frac{u_1^2}{2!}\right)\frac{d^2 f(u_0)}{du_0^2}, \end{aligned} \tag{7}$$

$$A_3 = u_3 \frac{df(u_0)}{du_0} + u_1 u_2 \frac{d^2 f(u_0)}{du_0^2} + \left(\frac{u_1^3}{3!}\right)\frac{d^3 f(u_0)}{du_0^3},$$

$$A_4 = u_4 \frac{df(u_0)}{du_0} + \left(u_1 u_3 + \frac{u_2^2}{2}\right)\frac{d^2 f(u_0)}{du_0^2} + \left(\frac{u_1^2 u_2}{2}\right)\frac{d^3 f(u_0)}{du_0^3} + \left(\frac{u_1^4}{4!}\right)\frac{d^4 f(u_0)}{du_0^4},$$

$$\vdots$$

Continuing this course, the other Adomian polynomials can be obtained, which are defined by the general explicit formulae:

$$A_n = \sum_{k=1}^{n} \frac{1}{k!} \frac{d^k f(u_0)}{du_0^k} \left(\sum_{p_1+\cdots+p_k=n} u_{p_1} \cdots u_{p_k} \right), \qquad n \geq 1 \tag{8}$$

By substituting Eq. (5) and Eq. (6) into Eq. (4), this gives the recursive equation for u_{n+1} in terms of $(u_0,u_1,\ldots,u_n)$:

$$u_{n+1} = -\int_0^t A_n(s, u_0(s), u_1(s), \cdots, u_n(s))ds, \qquad n \geq 0 \tag{9}$$

Each term u_n of the solution corresponds to a correction of a given order, and the solution itself is the sum given in Eq. (5).

2.2. Adomian decomposition method adapted to the Webb equation

The Webb equation is a nonlinear differential rate equation that can be nondimensionally expressed as:

$$\frac{d\sigma}{d\tau} = -\frac{\sigma(1+b\sigma)}{(R+\sigma)(1+\sigma)}, \qquad \sigma_0 = [S]_0 / K_{SS} \tag{10}$$

where $\sigma = [S]/K_{SS}$, $\tau = V_M t/K_{SS}$, and $R = K_S/K_{SS}$. As an illustration, I present the four-term decomposition method below for the Webb equation in the recursive relation as:

$$A_0 = f(\sigma_0) = \frac{\sigma_0(1+b\sigma_0)}{(R+\sigma_0)(1+\sigma_0)}$$

$$\sigma_1 = -\int_0^\tau A_0 dt = -\tau A_0$$

$$A_1 = \sigma_1 \frac{df(\sigma_0)}{d\sigma_0}$$

$$\sigma_2 = -\int_0^{\tau} A_1 d\tau = -\frac{1}{2}\tau A_1 \tag{11}$$

$$A_2 = \sigma_2 \frac{df(\sigma_0)}{d\sigma_0} + \left(\frac{\sigma_1^2}{2!}\right)\frac{d^2 f(\sigma_0)}{d\sigma_0^2}$$

$$\sigma_3 = -\int_0^{\tau} A_2 dt = -\frac{1}{3}\tau A_2$$

$$A_3 = \sigma_3 \frac{df(\sigma_0)}{d\sigma_0} + \sigma_1\sigma_2 \frac{d^2 f(\sigma_0)}{d\sigma_0^2} + \left(\frac{\sigma_1^3}{3!}\right)\frac{d^3 f(\sigma_0)}{d\sigma_0^3}$$

$$\sigma_4 = -\int_0^{\tau} A_3 dt = -\frac{1}{4}\tau A_3$$

The resulting nondimensional solution for σ(t) is given by the sum of:

$$\sigma(t) = \sigma_0 + \sigma_1 + \sigma_2 + \sigma_3 + \sigma_4 \tag{12}$$

which is actually a polynomial in t of the 4th-order with constant coefficients that can be evaluated for any time. The higher-order terms can be obtained in a similar fashion. The n-th derivative of Eq. (10) and the Adomian polynomials up to the n-th order can be generated in Wolfram Mathematica 8 using the code *D[s*(1+b*s)/((s+R)*(1+s)),{s,**n**}]* and the function *AdomianPolynomials[u_,F_,**n**_]:=CoefficientList[ExpandAll[Series[F[Sum[λ^ku[k],{k,**n**}]],{λ,0,**n**}]],λ]*.

The dimensional time-product concentration data can be further calculated using the following nth-order-term expressions of Eq. (14):

$$t = \frac{K_{SS}}{V_M}\tau \tag{13}$$

$$[P]_t = -K_{SS}\sum_{k=1}^{n}\sigma_k \tag{14}$$

where k is the order of a particular term.

3. COMPUTATIONAL SIMULATIONS

The simulated concentrations of the product *versus* time data were generated by computation using the direct model of Eq. (14) and the *FindRoot* code to Eq. (2) in the Wolfram Mathematica 8 computer program. Here, the numerical values of the kinetic parameters were

assigned from the literature for human butyrylcholinesterase (huBChE), for substrate inhibition [15] (with benzoylthiocholine (BzTCh); K_s = 3 μM; K_{ss} = 3000 μM, b = 0.3) and substrate activation [6] (with butyrylthiocholine (BTCh); K_s = 20 μM; K_{ss} = 1000 μM, b = 3). The curves shown in Figure 1 illustrate the deviations of the data generated by the computation using the direct model of the 4th-order term of Eq. (14) from the data evaluated by the *FindRoot* code to Eq. (2), for various initial substrate concentrations.

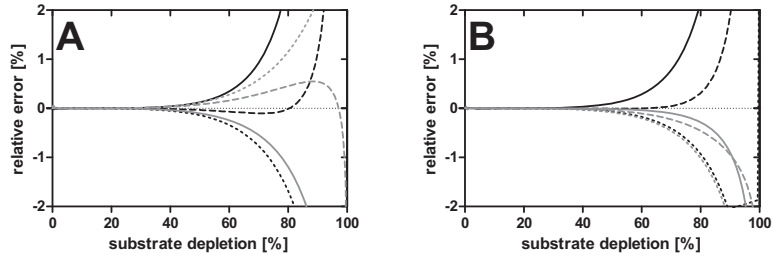

Figure 1. Comparisons of the various solution approaches (the 4th-order term of Eq. (14) *vs* the root-finding solution of Eq. (2)) for substrate inhibition (A) and substrate activation (B) in the huBChE reaction for various initial substrate concentrations. A. 3 μM (−), 7.5 μM (- -), 15 μM (···), 300 μM (−), 3000 μM (- -), 15000 μM (···). B. 20 μM (−), 50 μM (- -), 100 μM (···), 500 μM (−), 2000 μM (- -), 10000 μM (···).

It can be noted from Figure 1 that the approximated solutions evaluated with the Adomian decomposition method diverge from the true solutions as the substrate is consumed during the reactions. However, the relative errors of the calculated concentrations are 2% or less when the substrate concentrations do not decrease below 20% of their initial values. This means that efficient progress-curve data analysis can be carried out not only at the initial substrate concentrations, but also over the interval between this value and that at which around 80% of the initial substrate is converted to the product. As approximated solutions diverge most rapidly (most steeply) for the progress curves simulated with the lowest initial substrate concentrations (Figure 1), the same simulations were carried out using Eq. (14) with the higher-order terms (i.e., 5th, 6th, 7th and 8th orders). The results are shown in Figure 2, where it can be seen that higher-order terms in Eq. (14) improve the accuracy for wider substrate intervals (for up to 90% substrate consumption), although these higher-order terms demand more complex expressions and consequently more computational effort as the number of terms required for computation of the solution grows very rapidly with increasing

order in accordance with the Hardy-Ramanujam-Rademacher formula [2]. Hence, it appears that the explicit 4th-order term of Eq. (14) is already an useful alternative to the solutions computed with other numerical techniques. This can serve as a simple analytical tool for progress-curve analysis in standard curve-fitting programs, with an accuracy that is in the range of the usual experimental errors when up to 80% of the substrate is consumed in the reaction.

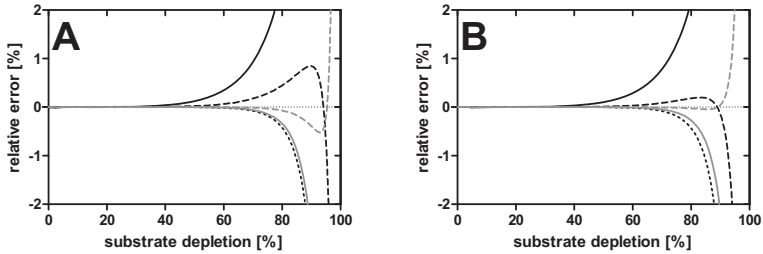

Fig. 2 Comparisons of the approximation solutions of the various orders for substrate inhibition (A) and substrate activation (B) in the human butyrylcholinesterase reaction, for the lower initial substrate concentrations (3 μM and 20 μM, respectively). A. 4th order (−), 5th order (**- -**), 6th order (···), 7th order (–), 8th order (- -). B. 4th order (−), 5th order (**- -**), 6th order (···), 7th order (–), 8th order (- -).

4. KINETIC PARAMETER ESTIMATION

Simulated progress-curve data for the cited huBChE [6,15] were generated by assigning the following numerical values, with respect to two different substrates, and consequently, kinetic behaviors: (1) inhibition with BzTCh: K_s = 3 μM; K_{ss} = 3000 μM, b = 0.3; and (2) activation with BTCh: K_s = 20 μM; K_{ss} = 1000 μM, b = 3. The solutions for the substrate concentrations as a function of time were generated by root-finding computation with the direct integrated Webb rate equation in Eq. (2) using the Wolfram Mathematica 8 computer program with the *FindRoot* code. More realistic experimental observation data were generated by introducing noise of a known type and magnitude into the simulated error-free concentration–time data. Normally distributed random errors were added to the exact substrate concentration calculated from Eq. (2) using the Mathematica software. The individual substrate concentration datasets were converted to product concentration profiles ($[P]_t = [S]_0 - [S]_t$). The time-courses that resulted (for the data that represent the substrate consumption for up to 80% of its initial value

at low concentrations; see Figure 3A, B) were used to estimate the kinetic parameters using the GraphPad Prism 5 software package.

The 4th-order term of the model approximation of Eq. (14) for product accumulation was also implemented in the GraphPad Prism 5 computer program for the calculation of the theoretical product concentrations, as a user-defined, built-in, explicit model equation (see Appendix B). This standard curve-fitting program has an all-user interface that allows users to easily handle global least-squares nonlinear regression curve fitting, to adjust the values of the model parameters to find the curve that best predicts the data.

The modeling results for huBChE substrate inhibition (with BTCh) and activation (with BzTCh) are shown in Figure 3A, B for each progress curve (solid lines), and the parameter estimates are given in Table 1.

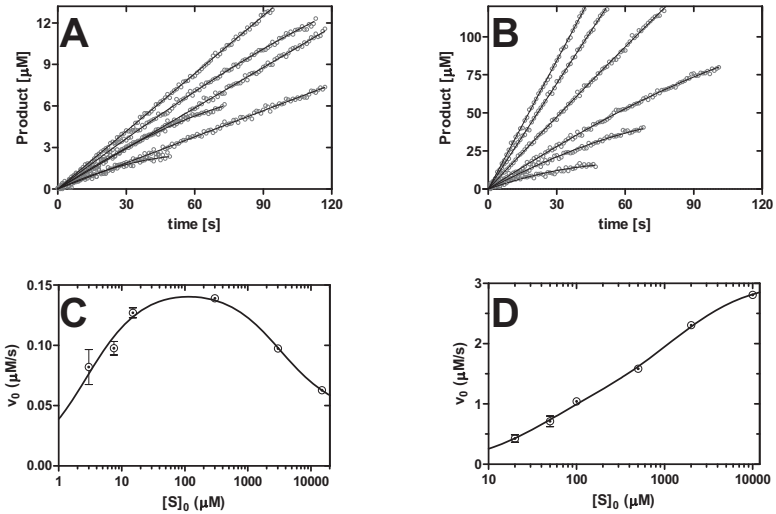

Figure 3. Simulated experimental time–product concentrations and initial-rate *versus* initial substrate concentration profiles for substrate inhibition (A, C) and substrate activation (B, D) in the huBChE reaction. The symbols represent the simulated data with added 'experimental noise', with the theoretical parameter values from the text and the following initial substrate concentrations: A, C. 3, 7.5, 15, 300, 3000 and 15000 μM. B, D. 20, 50, 100, 500, 2000 and 10000 μM. The lines are the theoretical concentrations obtained using the 4th-order term approximation of Eq. (14) (in A, B) and the initial rate values calculated using Eq. (1) (in C, D), and the estimated parameter values given in Table 1.

Table 1. Parameters acquired by global progress-curve and initial-rate fitting. Estimates for the kinetic parameters fitted to the data shown in Figure 3 that were obtained using the 4th-order term model approximation of Eq. (14) and initial rates of Eq. (1). Data are means ±SD.

Substrate	V_M(μM/s)	Ks (μM)	Kss (μM)	b
		Theoretical values		
BzTCh	0.150	3.00	3000	0.30
BTCh	1.00	20.0	1000	3.00
		Progress-curve fitting		
BzTCh	0.1498 ±0.0003	3.05 ±0.03	2989 ±45	0.304 ±0.002
BTCh	0.973 ±0.014	19.0 ±0.7	957 ±17	3.08 ±0.04
		Initial-rate fitting		
BzTCh	0.147 ±0.010	2.78 ±0.76	3300 ±2200	0.30 ±0.12
BTCh	1.27 ±0.21	40 ±13	1340 ±440	2.39 ±0.37

The initial rates were also determined by estimating the slopes of the tangents of each of the individual progress curves at the data intervals where less than 10% of the initial amounts of the substrate had been converted to product. The initial velocity *versus* substrate concentration profiles are shown in Figure 3C, D, and the parameter estimates obtained using Eq. (1) for the classical v_0 *vs* $[S]_0$ analyses are also given in Table 1. These analyses demand accurate initial velocity evaluations, which cannot be obtained in particular at low substrate concentrations (see Figure 3C, D).

The best parameter values shown in Table 1 yielded a surprisingly good fit to the experimental data of the model of Eq. (14) by applying standard nonlinear regression software, although only the 4th-order term approximations were used for the reaction data that represent less than 80% of substrate transformation in each progress curve. Thus, the results verify the correctness of the derived approximation solutions presented here. On the contrary, the initial-rate analyses lead to much greater uncertainties in the kinetic parameter estimates when fitting Eq. (1) to the v_0 *versus* $[S]_0$ data.

5. FURTHER MODIFICATIONS TO THE REACTION MODEL

It should also be emphasized that real-world enzymes generally do not obey the irreversible substrate-conversion mechanism, as proposed in the reaction model of this article (see

Scheme 1). Instead, the forward velocities of many enzyme-catalyzed reactions are affected by product inhibition if the enzyme or enzyme-substrate complex and product can form unproductive complexes, as illustrated in Scheme 2, although more realistic reactions are further reversible. The reversibility of the reaction is not the case for hydrolytic enzymes like the cholinesterases, although reports on human acetylcholinesterase product inhibition are known [16].

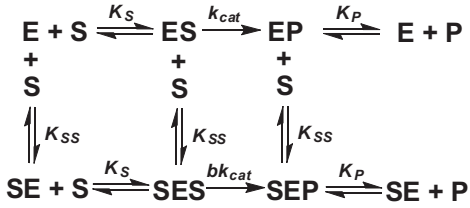

Scheme 2

However, also the extended rate equation that describes the kinetics of such product-inhibition mechanisms can be transformed into a Webb-type equation. Here, the net rate of substrate decay can be expressed as:

$$v = -\frac{d[S]}{dt} = \frac{\frac{V_M}{K_S}\cdot[S]\left(1+\frac{b}{K_{SS}}\cdot[S]\right)}{1+\frac{[S]}{K_S}+\frac{[S]}{K_{SS}}+\frac{[P]}{K_P}+\frac{[S]^2}{K_S K_{SS}}+\frac{[S][P]}{K_{SS}K_P}} \tag{15}$$

After considerable reformulation of Eq. (15), and taking mass balance (i.e., $[S]_0 = [S] + [P]$) into consideration, the net rate equation can be replaced with Eq. (16):

$$v = -\frac{d[S]}{dt} = \frac{\frac{V_M}{K_S}\cdot[S]\left(1+\frac{b}{K_{SS}}\cdot[S]\right)}{1+\frac{[S]_0}{K_P}+\frac{[S]}{K_S}+\frac{[S]}{K_{SS}}-\frac{[S]}{K_P}+\frac{[S]_0[S]}{K_{SS}K_P}+\frac{[S]^2}{K_S K_{SS}}-\frac{[S]^2}{K_{SS}K_P}} \tag{16}$$

which can be expressed in terms of the Webb-type form as:

$$v = -\frac{d[S]}{dt} = \frac{V_M^*[S]\left(1+b\frac{[S]}{K_{SS}}\right)}{\left(K_S^*+[S]\right)\left(1+\frac{[S]}{K_{SS}}\right)} \tag{17}$$

where:

$$V_M^* = \frac{V_M / K_S}{\left(1/K_S - 1/K_P\right)} \tag{18}$$

and:

$$K_S^* = \frac{\left(1 + [S]_0 / K_S\right)}{\left(1/K_S - 1/K_P\right)} \tag{19}$$

An interesting feature of Eq. (17) is that the apparent limiting rate V_M* and dissociation constant K_S* can have negative values if $K_S > K_P$, although they must both have the same sign. However, in any case, the Adomian decomposition method can also be used to find the approximated solutions of such modified Webb rate equations.

6. CONCLUSIONS

The most elegant and ideal simplification of kinetic-parameter evaluation from time-course data can be performed when the algebraic integration of the rate equation results in an explicit mathematical equation that describes the kinetics of the reaction model. However, exact integrated rate equations can be considered as simple and useful alternatives to the widely used numerical integration approach, although only for enzymes that obey the generalized Michaelis-Menten reaction mechanism [10-12], as integrated rate equations do not exist in closed forms for more complex reaction mechanisms.

Hence, in this article, I have presented the approximated solutions of the Webb rate equation using the Adomian decomposition method, which can help in the identification of kinetic parameters for the kinetics of cholinesterase substrate inhibition/ activation. The procedure demonstrated here offers an easy and quick analysis of progress curves of enzymatic reactions within the framework of the Webb model (e.g. cholinesterases), to extract the kinetic parameters without relying on specialized algorithms and software. The suggested approximations to the solution of the Webb equation can be correctly written and saved as user-defined, built-in equations in optional nonlinear regression computer programs. This is an improvement that can greatly facilitate the characterization of enzyme kinetics in various areas across life-sciences research.

ACKNOWLEDGEMENTS

This study was supported by the Slovenian Research Agency (grant P1-170).

APPENDIX A

Inspection of the differential Eq. (1) shows that its variables of time t and substrate concentration [S] can be separated as:

$$V_M dt = -\frac{\left([S]+K_S\right)\left([S]+K_{SS}\right)}{[S]\left(b[S]+K_{SS}\right)}d[S] = -\left(\frac{1}{b}+\frac{K_S}{[S]}+\frac{(b-1)\left(K_{SS}-bK_S\right)}{b\left(b[S]+K_{SS}\right)}\right)d[S] \qquad (20)$$

and direct integration of the expression that results gives the integrated Webb equation in the implicit form of Eq. (2).

APPENDIX B

Software-user-defined, built-in equations using 4th-order term approximations of solutions for product concentrations in GraphPad Prism 5.

```
s=S0/Kss
R=Ks/Kss
t=Vm*x/Kss
sR=(s+R)*(1+s)
f0=s*(1+b*s)/sR
f1=((-1+b)*s^2+R*(1+b*s*(2+s)))/sR^2
f2=-(2*(-(-1+b)*R^2+(-1+b)*s^3+R*(1+3*s+3*b*s^2+b*s^3)))/sR^3
f3=6*((1-b)*R^3+(b-1)*s^4-(b-1)*R^2*(1+4*s)+R*(1+4*s+6*s^2+4*b*s^3+b*s^4))/sR^4
s1=-t*f0
s2=-(t/2)*s1*f1
s3=-(t/3)*(f1*s2+f2*s1^2/2)
s4=-(t/4)*(f1*s3+f2*s1*s2+f3*s1^3/6)
Y=-Kss*(s1+s2+s3+s4)
```

REFERENCES

[1] M. Goličnik, On the Lambert W function and its utility in biochemical kinetics, *Biochem. Eng. J.* **63** (2012) 116-123.

[2] J. R. Sonnad, C. T. Goudar, Solution of the Michaelis-Menten equation using the decomposition method, *Math. Biosci. Eng.* **6** (2009) 173-188.

[3] G. Gonzales-Parra, L. Acedo, A. Arenas, Accuracy of analytical-numerical solutions of the Michaelis-Menten equation, *Comp. Appl. Math.* **30** (2011) 445-461.

[4] J. R. Sonnad, C. T. Goudar, Solution of the Haldane equation for substrate inhibition enzyme kinetics using the decomposition method, *Math. Comp. Model.* **40** (2004) 573-582.

[5] Z. Radić, N. A. Pickering, D. C. Vellom, S. Camp, P. Taylor, Three distinct domains in the cholinesterase molecule confer selectivity for acetyl- and butyrylcholinesterase inhibitors, *Biochemistry* **32** (1993) 12074-12084.

[6] P. Masson, P. Legrand, C. F. Bartels, M. T. Froment, L. M. Schopfer, O. Lockridge, Role of aspartate 70 and tryptophan 82 in binding of succinyldithiocholine to human butyrylcholinesterase, *Biochemistry* **36** (1997) 2266-2277.

[7] E. Reiner, V. Simeon-Rudolf, Cholinesterase: substrate inhibition and substrate activation, *Pflügers Arch – Eur. J. Physiol.* **440** (2000) R118-R120.

[8] J. L. Webb, *Kinetics of Some Complex Enzyme Reaction Types*, Academic Press, New York, 1963.

[9] M. V. Putz, On the reducible character of Haldane-Radić enzyme kinetics to conventional and logistic Michaelis-Menten models, *Molecules* **16** (2011) 3128-3145.

[10] S. Schnell, C. Mendoza, Closed-form solution for time-dependent enzyme kinetics, *J. Theor. Biol.* **187** (1997) 207-212.

[11] M. N. Berberan-Santos, A general treatment of Henri-Michaelis-Menten enzyme kinetics: exact series solution and approximate analytical solutions, *MATCH Commun. Math. Comput. Chem.* **63** (2010) 283-318.

[12] M. Goličnik, Die Kinetik der Invertinwirkung" of L. Michaelis and M. L. Menten revisited after 100 years: closed-form solutions of genuine invertase-reaction dynamics, *MATCH Commun. Math. Comput. Chem.* **70** (2013) 63-72.

[13] G. Adomian, *Solving Frontier Problems of Physics: The Decomposition Method*, Kluwer, Boston, 1994.

[14] J. M. Younker, Numerical integration of the chemical rate equations via a discretized Adomian decomposition, *Ind. Eng. Chem. Res.* **50** (2011) 3100-3109.

[15] P. Masson, B. N. Goldstein, J. C. Debouzy, M. T. Froment, O. Lockridge, L. M. Schopfer, Damped oscillatory hysteretic behavior of butyrylcholinesterase with benzoylcholine as substrate, *Eur. J. Biochem.* **271** (2004) 220-234.

[16] T. Szegletes, W. D. Mallender, P. J. Thomas, T. L. Rosenberry, Substrate binding to the peripheral site of acetylcholinesterase initiates enzymatic catalysis. Substrate inhibition arises as secondary effect, *Biochemistry* **38** (1999) 122-133.